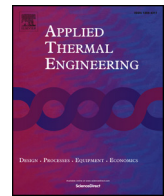




ELSEVIER

Contents lists available at ScienceDirect

Applied Thermal Engineering

journal homepage: www.elsevier.com/locate/apthermeng

Detection and classification of lean blow-out and thermoacoustic instability in turbulent combustors



Chandrachur Bhattacharya^{a,b}, Somnath De^c, Achintya Mukhopadhyay^c, Swarnendu Sen^c,
Asok Ray^{a,d,*}

^a Department of Mechanical Engineering, The Pennsylvania State University, University Park, PA 16802, USA

^b Department of Electrical Engineering, The Pennsylvania State University, University Park, PA 16802, USA

^c Department of Mechanical Engineering, Jadavpur University, Kolkata 700 032, India

^d Department of Mathematics, The Pennsylvania State University, University Park, PA 16802, USA

HIGHLIGHTS

- The FFT-based method computes a scalar measure to distinguish between the operational regimes of a combustor.
- The scalar-valued measure shows applicability in the early detection of imminent changes to LBO or TAI.
- The proposed algorithm uses audio data from a non-intrusive and inexpensive external microphone.

ARTICLE INFO

Keywords:

Thermoacoustic instability
Lean blow-out
FFT-based analysis
Turbulent combustion systems

Abstract: Lean blow-out (LBO) and thermoacoustic instability (TAI) are common undesirable occurrences in modern lean-burn turbulent combustion systems, such as fossil-fuel furnaces for gas turbines and in both land-based power generation and marine or aviation propulsion applications. While LBO causes loss of power due to flame extinction, TAI leads to loud noise, vibrations and mechanical fatigue-failure. Timely detection and classification of the operating conditions are important for both open-loop and closed-loop control of combustion systems to ensure their long service life, high efficiency, and reliability & availability. Data-driven techniques already exist for detection of these phenomena; however, most of these techniques require high training and/or processing times. This paper presents a fast Fourier transform (FFT)-based method to generate, in real time, a single scalar-valued measure for detection and classification of operational regimes; this measure can also be used to identify precursors (i.e., for prediction of impending LBO and TAI). This FFT-based method utilizes prior knowledge of the combustion system acoustics; and the measure acts as a classifier to distinguish different operational regimes. The underlying algorithms have been validated on time series data, collected from a (commercially available) microphone sensor that is external to the laboratory-scale experimental apparatus.

1. Introduction

The rising concerns of global warming and environmental hazards due to combustion of fossil fuels have brought about significant changes in the energy portfolio with a progressively increasing shift towards utilization of renewable sources of energy. The increasing capacity of power generation, based on renewable (e.g., solar and wind) energy, is fast transforming the role of thermal power plants to that of on-demand peak load plants [1]. However, the unpredictable availability of energy sources like the sun and wind would require thermal power plants to be designed to compensate for fluctuations in the power generated from

renewable sources. Consequently, intermittent operations with large fluctuations in the plant load would require the combustors to be designed with high turn-down ratios. High turn-down ratios have also been a requirement for burners in fuel-fired furnaces in process industries and manufacturing applications due to large differences in the energy and power requirements in different processes or even different stages of a manufacturing process like heating and holding phases of annealing of materials. Even for locomotion needs, the primary energy source is still the combustion of fossil fuels in furnaces or gas turbines.

The need for reduction in carbon footprint and efforts towards achieving carbon neutrality have led to exploration of newer grades of

* Corresponding author at: Department of Mechanical Engineering, The Pennsylvania State University, University Park, PA 16802, USA.

E-mail address: axr2@psu.edu (A. Ray).

<https://doi.org/10.1016/j.applthermaleng.2020.115808>

Received 18 April 2020; Received in revised form 2 July 2020; Accepted 24 July 2020

Available online 03 August 2020

1359-4311/ © 2020 Elsevier Ltd. All rights reserved.

fuel, especially those obtained from biological sources. Apart from the low heating values and low flame speeds in many of these fuels, like biogases (which contain a large proportion of carbon-dioxide), there are wide variations in the fuel composition itself, depending on its source. Furthermore, combustion systems are also often operated under fuel-lean conditions to ensure operation at lower temperatures, thus mitigating emission of oxides of nitrogen (NO_x).

Large turn-down ratios, a wide range of fuel compositions leading to large variations in the flame speed, and the need to operate under a large range of equivalence ratios from fuel rich to fuel-lean conditions make modern combustion systems susceptible to the following two major anomalous phenomena.

1. *Lean-blow out (LBO)*: LBO, which is a phenomenon that occurs when the flame is lean, causes loss of flame, possibly leading to complete loss of power in the combustion system, which may be difficult to reignite; and
2. *Thermoacoustic instability (TAI)*: TAI may occur due to a constructive interference between heat release rate and acoustically-driven flow perturbation in combustors [2], assisted by the fact that these systems have very low acoustic damping [3]. Although it is possible to occasionally encounter TAI in lean conditions, TAI is treated as a phenomenon occurring at high equivalence ratios, close to or higher than stoichiometric; this assertion is based on the experimental observations conducted on the apparatus reported in this paper. In general, TAI leads to loud noise and vibrations, due to the high energy in the system, which can be harmful to structural integrity of the combustor due to thermomechanical fatigue-failure. In extreme cases, total breakdown of the system may occur if the frequency of the generated thermoacoustic waves matches the natural frequency of the system. This phenomenon may also cause flow reversal and choked flow, leading to flame instability and extinction in through-flow combustors [4,5].

Thus, for mitigation of the above undesirable phenomena and life extension of the combustion system, early prediction of forthcoming LBO and TAI is necessary to ensure that an appropriate decision and control action can be taken to reduce the probability of their occurrence.

The problems of LBO and TAI detection and prediction have been studied extensively in recent years and several techniques already exist, which use time series data or video data. The main idea here is the preemptive detection of imminent LBO and TAI so that decision and control actions can be taken prior to their occurrence.

Lefebvre [6] introduced the concept of correlation function-based LBO prediction, which is useful for combustor design, but it may not be sufficiently accurate for online LBO prediction and control. Since then OH* and CH* chemiluminescence has been used by researchers [7,8] to study and detect LBO in swirl-stabilized combustors. Based on the facts that there are localized flame extinction and re-ignition near LBO, and the flame detaches from and re-attaches to the burner, Yi and Gutmark [9] have reported that “*near-lean-blowout combustion is characterized by the intensified, low-frequency combustion oscillations of the OH* signal, (typically, below 30 Hz).*” This observation has been since augmented to be used on a pulse combustor using ion current sensors [10]. More recently, Chang et al. [11] compared the standard practice of using CH* signals to generate “*normalized root mean square (NRMS), normalized cumulative duration (θ) and fraction of the fast Fourier transform (FFT) power at low frequencies*” to study the precursors to LBO and they proposed a new threshold-based metric to improve upon the same. Other researchers (e.g. [12]) have used the changing flame color as a precursor to LBO. It is noted that, in the lean limit, the flame color changes from red to blue; and using a commercial color charge-coupled device (CCD) camera, a good estimate of approaching LBO can be obtained. In other works [13], chemiluminescence data have been used for recurrence analysis to detect LBO.

Similar to LBO, it is necessary to have a real-time method for prediction of TAI onset. Since it is not desirable to allow the combustion system to enter into the unstable regime of operation, early prediction and real-time control of TAI phenomena have been studied in literature by using various techniques. For example, Nair et al. [14] have shown that, during lean operation, as the combustor goes unstable, the pressure trace exhibits ordered (e.g., nearly sinusoidal) oscillations. During nominal conditions (i.e., stable operations), however, the pressure time series shows a chaotic signature. Murugesan and Sujith [15] extended this idea by using a visibility graph technique to convert the pressure time series into a complex network [16] and to show that combustion noise is scale-free; it transitions to an ordered signal during instability and achieves a limit-cycle-like behaviour. This approach has been recently used in combination with machine learning approaches to do an experimental study of TAI [17]. Recurrence analysis for dynamic characterization of TAI in a ducted inverse-diffusion flame is another approach [18]. Mondal et al. [19] introduced a simpler and faster FFT-based dynamic characterization, which yields results comparable to those of the visibility graph technique. The concept that the ordered nature of the pressure signal implies a lower data entropy [20] during unstable operation, as compared to the stable operational regime, has been used by researchers for the online prediction of TAI [21]. Sarkar et al. [22] used hi-speed flame image data for early prediction of impending instability using neural networks. More recently hidden Markov models [23] have been used by researchers to detect and predict the onset of TAI [24].

Most of the above techniques, which have been validated in a laboratory environment, may not be easy to implement at industrial installations, because of the following reasons: (i) computational overhead and/or (ii) difficulties in interpretation of the metrics due to limited familiarity of the engineers with these techniques. On the other hand, FFT has been used for studying dynamic signals for a long time and hence techniques based on FFT can be more suitable for easy implementation. Moreover, a majority of the sensors (e.g. pressure sensors, OH* sensors, and cameras), required for the above analysis, are expensive and, in some cases like pressure sensors, may often need direct access on the combustor. Placement of such sensors is difficult and is often not possible in actual combustion systems (and even experimental rigs); especially, adequate optical access (for optical sensors) which may not always be available in combustors. It is, thus, necessary to have sensors, which are simple, inexpensive and can capture the combustor dynamics without any major modifications of its design or construction.

This paper proposes an FFT-based detection technique that incorporates a combination of the domain knowledge as well as basic characteristics of the physical system, which significantly reduces the computational complexity of the data-driven technique. The main idea here is a major extension of the previous work by Mondal et al. [19], which used an FFT-based method to discriminate between stable combustion signals and those that are undergoing thermoacoustic instability and showed that it gives results comparable to the visibility graph technique. The modified method, proposed in the current paper, has been tested on the audio time series of a microphone placed near a combustor apparatus; the results show that the extended algorithm is capable of discriminating stable, TAI, as well as pre-LBO signals.

The proposed method of LBO and TAI detection relies on the knowledge of dominant acoustic modes. This information can be often generated experimentally on test rigs; and if that is not possible, usage of one or more of several analytical methods is recommended, where the dominant acoustic modes can be identified by using Helmholtz models or Flame transfer functions (FTFs). In this regard, several papers have reported the results of theoretical and numerical analysis of dominant acoustic modes. For example, Hosseini et al. [25] identified the modes in a Rijke tube, while analyses of a premixed combustor [26] and a swirling flame [27] were reported by other researchers. A very thorough theoretical study on the acoustic modes, including azimuthal

modes in annular combustors is available in [28].

The time-series to be analyzed is obtained from the audio signal that is recorded with a commercially available microphone (as compared to pressure signals obtained from expensive and intrusive pressure sensors as in [19]). This microphone is placed at a distance of about 60 cm from the experimental combustor and records a mono-channel audio signal.

Contributions: Major contributions of the paper are summarized below.

1. *Computer-instrumented sensor software:* The software sensor replaces expensive and bulky sensor hardware (e.g., pressure sensors, imaging cameras, or other optical sensors) that requires direct or optical access to the combustor. In contrast, the software sensor only requires a commercially available microphone placed at a distance from the combustion system.
2. *Development of a scalar-valued measure derived from time series of sensor data:* This measure is computed in real time by a synergistic combination of FFT-based analysis and domain knowledge to identify LBO, TAI, and stable operations in a pre-mixed combustor from audio time-series.
3. *Experimental validation of the concept:* The efficacy of the proposed algorithm has been validated with experimental data from a laboratory scale combustion apparatus.

Organization of the paper: The paper is organized in five sections including the current section. Section 2 describes the laboratory-scale combustor apparatus and the experimental methodology. Section 3 outlines the theory of the FFT-based algorithm, while Section 4 presents the results generated by the algorithm on the time-series data, collected from the experimental apparatus. Section 5 summarizes and concludes the paper along with a few recommendations for future research.

2. Experimental apparatus and methodology

The combustor apparatus, as depicted in Fig. 1, has four main components: (a) a premixing chamber; (b) a combustion chamber; (c) an exhaust section; and (d) a microphone with a computer-instrumented and computer-controlled data acquisition system (DAQ). The premixing chamber consists of five sets of fuel inlets at five different axial locations and an air inlet further upstream. The air port is located 20 mm downstream of the bottom end of the premixer tube. In this study, the fuel ports furthest from the combustion chamber are used, located at 330 mm upstream of the dump plane [12]. This ensures

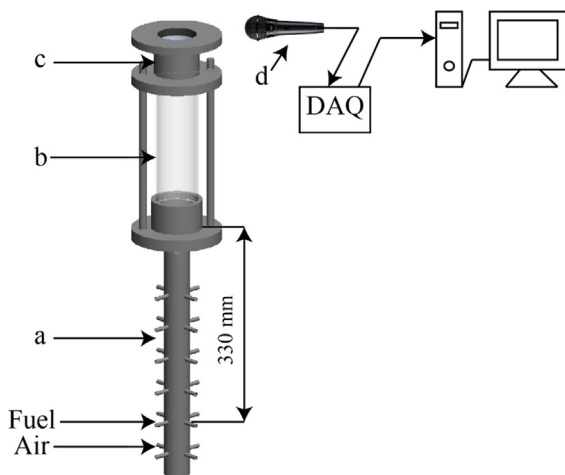


Fig. 1. Experimental apparatus showing different components: (a) premixing section; (b) combustion chamber; (c) exhaust chamber; and (d) a microphone with a computer-instrumented and computer-controlled data acquisition system (DAQ) to capture the acoustic signal from flame.

a nearly premixed mixture at the dump plane. Fig. 1 further shows that each fuel or air port has four inlets positioned circumferentially (90° degree apart from each other) on the premixing tube. This type of arrangement for air and fuel locations reduces the circumferential asymmetry in the flow configuration. A swirler (swirl number, SN = 1.26) with blade angle of 60° is present 15 mm upstream of the dump plane causing the formation of re-circulation zones to enhance the flame stability. The combustion chamber comprises of a quartz tube 200 mm in length, having an outer diameter of 65 mm, which provides the optical access to the turbulent flame. Downstream of the combustion chamber, an exhaust section of 50 mm length and 60 mm inner diameter is fitted on the quartz tube. In this configuration, the combustion system is open to atmosphere allowing the burnt gases to escape. The combustor apparatus that has been used in the current investigation had also been used in several previous research publications (e.g. [12]) and the readers are referred to these papers for more details on this apparatus.

The air flow rate (\dot{Q}_A) is metered using an Alicat MFC (MCR Series, Range: 0–1500 SLPM) and the fuel flow rate (\dot{Q}_F) is metered using another Alicat MFC (MCR Series calibrated for LPG, Range: 0–250 SLPM). Here SLPM is *standard liter per minute* which is a unit of volumetric flow rate of a gas at standard conditions for temperature and pressure (STP). Thus, using the mass flow rates of the air and fuel (\dot{M}_A and \dot{M}_F , respectively), the global equivalence ratio (ϕ) calculated as $\left(\phi = \left(\frac{\dot{M}_A}{\dot{M}_F}\right)_{\text{stoichiometric}} / \left(\frac{\dot{M}_A}{\dot{M}_F}\right)_{\text{actual}}\right)$, can be varied. The fuel used in these experiments was LPG gas (~60% butane and ~40% propane), the composition of which is specified by the manufacturer [29].

In an effort to capture the dynamics of a premixed flame, audio data have been acquired using a microphone (Philips SBCMD110/01) with a maximum audio sampling rate of 44 kHz [30]. The objective here is to record the sound produced by the combustion system at different equivalence ratios; the microphone is placed at a distance of 60 cm from the combustor. The audio interface (*Acquire Sound VI*) of the National Instruments software, LabVIEW 2018, acts as the data acquisition (DAQ) system, where the audio signal from the microphone is supplied to the DAQ using the standard inbuilt 3.5 mm auxiliary jack. The microphone data are recorded for a specified time duration (see SubSection 4.1) at the sampling frequency (f) of 12 kHz. The recorded output signal is represented in 16 bits and is auto-normalized to arbitrary units with a range of ± 1 .

3. Fast Fourier Transform (FFT) algorithm

This section develops a fast Fourier transform (FFT)-based algorithm that forms the backbone of the data-driven method for detection and classification of LBO and TAI.

3.1. Previous work

Mondal et al. [19] proposed a fast Fourier transform (FFT)-based method for discrimination between stable and unstable combustion operation, where they defined the following two metrics by using pressure time series from an experimental combustor at Penn State [31].

- *Metric A* is obtained as the ratio of the energy content of the dominant frequency (i.e., the frequency corresponding to the maximum amplitude in the power spectrum) to the energy content of the second most dominant frequency that is a non-harmonic of the dominant frequency was computed. The rationale is that combustion instability causes excitation of harmonics of the unstable mode and thus, most of the signal energy is concentrated in the unstable mode and its harmonics. This ratio is expected to be higher for an unstable signal than for a stable signal, because a stable combustion system resembles a near-uniform distribution of energy over the

entire spectrum. *Metric A* classified a signal as unstable if the ratio was greater than a specified threshold.

- *Metric B* is the ratio of the energy content at the dominant frequency to the total energy content of the signal. The unstable signals have a significant energy in the excited dominant frequency. Thus, *Metric B* classifies a signal as unstable if the ratio is greater than the specified threshold.

3.2. The proposed FFT-based algorithm

The algorithm proposed by Mondal et al. [19] is limited by the fact that it is capable of distinguishing only between statistically stationary time series (over a complete window length of 8 s) that are either completely stable or undergoing TAI. It is unable to detect LBO, and is not adaptable for online detection of transient data using small data windows. However, in a real combustor, it would be necessary to detect LBO too, and thus the objective would be to create a simple measure that could distinguish TAI, LBO and stable operations in an online fashion.

Thus, a modified methodology is necessary to attain the above objective. During the course of experimentation, it was observed that the system showed any one of the two dominant frequencies during TAI, namely ~190 Hz and ~520 Hz in the ranges of ± 20 Hz and ± 40 Hz, respectively. Similarly during the onset of LBO, the frequencies showing the maximum amplitude were ~50 Hz (± 5 Hz) and ~100 Hz (± 10 Hz). Compared to these observations, the stable operation was more broadband in nature as seen in the FFT spectrum. System-specific metrics can now be defined based on this knowledge of the system characteristics.

As the dominant frequencies during either LBO and TAI are mostly in the ranges of 50 ± 5 Hz, 100 ± 10 Hz, 190 ± 20 Hz and 520 ± 40 Hz, the algorithm first recognizes the most dominant frequency in each of these four frequency ranges by observing which frequency (from each range) has the highest magnitude in the FFT spectrum. The FFT itself is restricted to a cover of 10 Hz to 1200 Hz, with an upper limit more than double of the dominant frequency range observed during TAI. Higher frequencies yield no major information about the state of the system.

For each locally maximum frequency, the power (denoted as $power_{freq}$) is used to compute the energy 'stored' in that frequency mode from the area under the FFT around that frequency. This energy is assumed to be akin to a measure of the energy contained in that particular mode, similar to *Metric B* used in [19]. For computing the area, a bandwidth support of ± 5 Hz is assumed. Following this procedure, four values of frequency powers are computed corresponding to the four dominant frequencies indicated as $power_{50}$, $power_{100}$, $power_{190}$ and $power_{520}$, where each of the (positive) peak powers is normalized to maximum value of 1. The rationale for taking this approach is as follows.

When any one of the frequencies dominates, the respective individual power is higher than that of the rest, because most of the energy is concentrated around the dominant frequency mode. Similarly, when a modal frequency does not dominate, its power is relatively low. Finally, to serve as a (scalar-valued) measure, an overall ratio (denoted as ρ) is defined as follows:

$$\rho \triangleq \frac{(1 - power_{50}) \times (1 - power_{100})}{(1 - power_{190}) \times (1 - power_{520})} \quad (1)$$

where $power_n \in (0, 1)$, $n = 50, 100, 190, 520$.

By virtue of its construction, the value of ρ in Eq. (1) is low when either or both of the 50 Hz or 100 Hz frequencies dominate, i.e. the system is approaching LBO. This is so, because high values of power peaks in LBO (e.g., $power_{50}$ and/or $power_{100}$) lead to a small value of the numerator and simultaneously low values of power peaks in TAI (e.g., $power_{190}$ and $power_{520}$) lead to relatively high values of the denominator in Eq. (1); hence this situation of LBO yields a low value of the scalar

measure ρ . By a similar argument, high values of ρ are generated if either one or both of 190 Hz and 520 Hz frequencies dominate, i.e., the system is approaching or undergoing TAI. Intermediate values of ρ would indicate stable operations, i.e., neither TAI nor LBO. Appropriate thresholds, θ_1 and θ_2 , can now be assigned for detection of LBO and TAI respectively on the scalar ρ , in an attempt to distinguish among LBO, TAI, and stable operations of the experimental combustor solely based on the audible sound, emitted by the system.

In view of the above explanation, the thresholds, θ_1 and θ_2 , for detection and prediction of LBO and TAI respectively, have been identified by using the Bayes' criterion of minimum average cost [32] from a jointly optimal threshold set. In the operation of combustion systems, it is safer to have false alarms, i.e., classifying stable operations as unstable (i.e., LBO and TAI) rather than to have misclassifications of unstable as stable. In this paper, the relative cost of misclassifications of stability are made twice those of false-alarms of LBO and TAI.

4. Results and discussions

This section analyzes the data collected from the experimental apparatus, described in Section 2 by using the algorithms explained in Section 3. The experimental procedure is described in SubSection 4.1 while an overview of the experimental observations is reported in SubSection 4.2 with the detailed results of the analysis presented in SubSections 4.3 and 4.4.

4.1. Experimental procedure

The experiments were conducted for different values of the equivalence ratio (ϕ) (see Section 2), starting at a lean condition and then increasing the equivalence ratio progressively until a very rich region of about $\phi = 2$ was reached. Subsequently, ϕ was reduced to very low values and, in some cases, the experiments were continued until LBO was reached.

During each experiment, the air flow rate (\dot{Q}_A) was held constant and the equivalence ratio (ϕ) was varied by changing the fuel flow rate (\dot{Q}_F) with the Alicat controller described in Section 2. For every experimental trail, each value of ϕ was maintained for 10 s during which the audio signal generated by the combustion system was recorded via the microphone-DAQ-LabView arrangement as detailed in Section 2.

The experimental observations are reported in SubSection 4.2. In order to allow for stationary observations, the system was allowed to stabilize for 30 s after each progressive change in \dot{Q}_F . This procedure ensured that no transient behavior was captured for steady state analysis in SubSection 4.3. For the few unsteady cases recorded in SubSection 4.4, a similar overall procedure was followed with the air-flow rate (\dot{Q}_A) held constant over the experiments with the fuel flow rate (\dot{Q}_F) being increased or decreased progressively every 10 s with Alicat's automatic flow-rate scheduling algorithm. The audio signals were recorded over the range of ϕ that was intended to be observed (generally 60 s having 6 values of ϕ per observation). The increments or decrements were intentionally kept small ($\Delta\phi \sim 0.035$) so as not to have strong transient fluctuations at the change points.

In this paper, neither flame images nor chemiluminescence data have been used for regime identification, because the motivation here is the development of a low computational-cost method for regime detection using inexpensive and non-invasive tools. For the purpose of illustration, some of these flame images are shown in Fig. 2, which were recorded at varying values of equivalence ratio (ϕ) ranging from stoichiometric to LBO. There are several published works by the authors of this paper (e.g. [12]), where the details are reported.

4.2. Experimental observations

A total of 112 steady-state 10-s long experimental observations were recorded. Of these, 39 observations corresponded to stable, 63 to TAI,

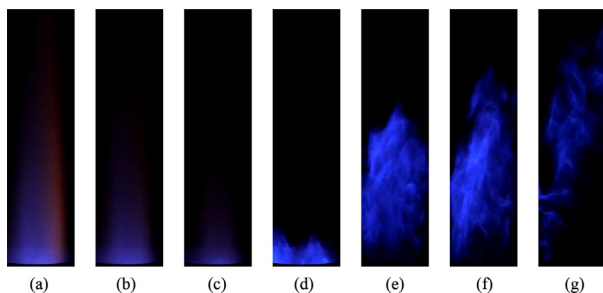


Fig. 2. Flame images showing the behavior of the flame at 7 different operating conditions between stoichiometric and LBO. The equivalence ratios are: (a) $\phi = 1.0$ (Undergoing TAI), (b) $\phi = 0.825$, (c) $\phi = 0.75$, (d) $\phi = 0.637$, (e) $\phi = 0.60$, (f) $\phi = 0.562$ and (g) $\phi = 0.50$ (Just prior to LBO).

and 10 to pre-LBO and LBO operations. The experiments showed the following observations:

- (i) Occurrence of TAI for richer ϕ close to or greater than stoichiometric; and
- (ii) Occurrence of LBO for low values of ϕ .

A distinct tonal sound was heard during TAI, which was also captured by the microphone. Similarly, pre-LBO regions were discerned by a fluttering in the flame and a very low-frequency growl. These observations, tallying the sound clip to the physical manifestation as well as the expected regime (compared to previous works [12,13]), were noted. These results have been used as the ground truth for validating the proposed FFT-based algorithm.

Figs. 3–5 show representative time-series and FFT plots for each of the three regimes, namely, pre-LBO, stable, and TAI; each figure consists of three plates, where the top left plate shows the audio time-series signal for the entire 10-s (steady-state) recording, the top right plate shows the FFT corresponding to that signal, and the bottom plate shows ‘zoomed in’ versions of the audio signals illustrating a 0.2-s window of the recording. A more detailed discussion of these findings are provided in the subsequent SubSections 4.3 and 4.4.

4.3. Steady-state signal analysis

This subsection analyzes statistically stationary data, where a given time series is expected to remain stationary at constant values of air and fuel flow rates, and thus the regime of operation appears to be similar

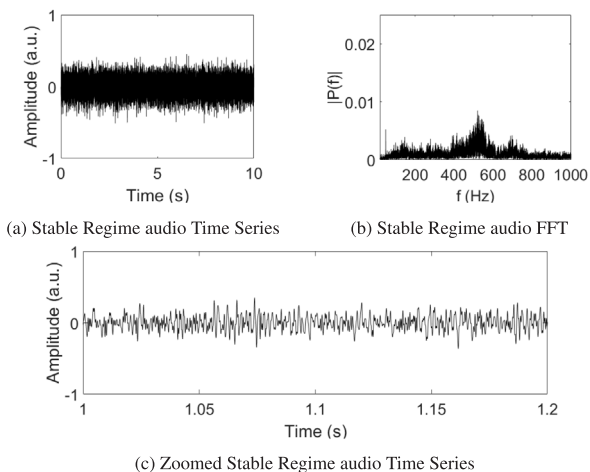


Fig. 3. Representative time series signals and FFT for stable regime, where “a.u.” in the ordinate of plots (a) and (c) indicates arbitrary units. ($\dot{Q}_A = 80SLPM$, $\dot{Q}_F = 2.4SLPM$, $\phi = 1.04$).

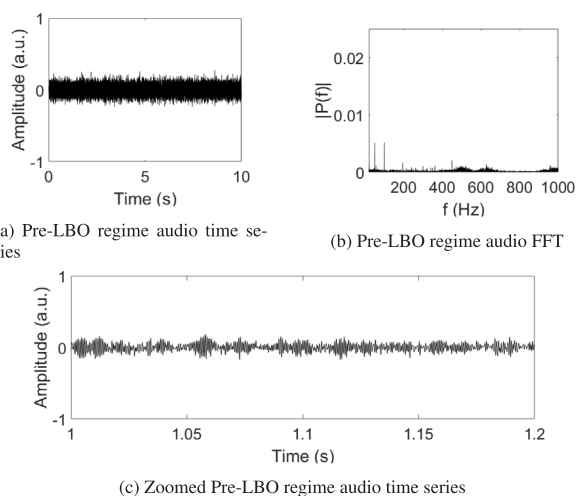


Fig. 4. Representative time series signals and FFT for LBO Regime, where “a.u.” in the ordinate of plots (a) and (c) indicates arbitrary units. ($\dot{Q}_A = 80SLPM$, $\dot{Q}_F = 1.1SLPM$, $\phi = 0.48$).

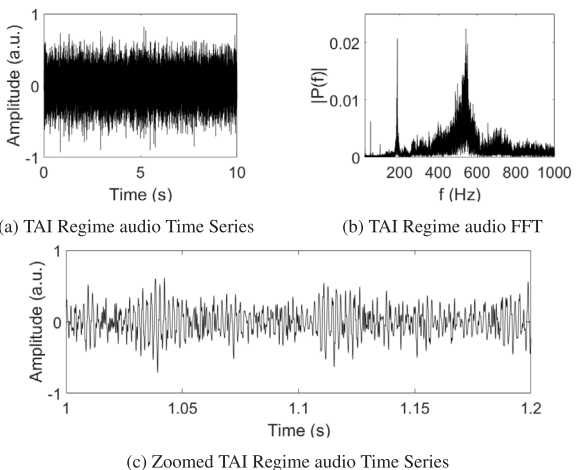


Fig. 5. Representative time series signals and FFT for TAI Regime, where “a.u.” in the ordinate of plots (a) and (c) indicates arbitrary units. ($\dot{Q}_A = 80SLPM$, $\dot{Q}_F = 2.8SLPM$, $\phi = 1.21$).

over the entire 10-s observation window.

In plotting the FFTs of the entire 10-s data, the dominance of the 50 Hz and 100 Hz frequencies can be distinctly seen in the pre-LBO case of Fig. 4b albeit with lower magnitudes, while strong peaks in the vicinity of ~190 Hz (188 Hz precisely) and ~520 Hz (542 Hz precisely) are seen during TAI in Fig. 5b. In contrast, the stable case of Fig. 3b shows a more broadband behavior in the spectrum as expected. It is also seen by comparison that the signal appears to have the highest amplitudes for TAI in Fig. 5a, intermediate for stable operation in Fig. 3a, and lowest during the pre-LBO regime in Fig. 4a. The rationale for not using the amplitude of the signal as a classification measure is described later in this subsection. The ‘zoomed-in’ segments of the audio time-series signals show:

- (i) Small-amplitude chaotic signals [14] under stable operation (Fig. 3c);
- (ii) Small-amplitude disordered oscillations in the pre-LBO regime (Fig. 4c); and
- (iii) Large-amplitude ordered signals in the TAI regime (Fig. 5c).

Using the Bayes’ criterion of minimum average cost on the entire ensemble of data, two thresholds θ_1 and θ_2 are assigned and evaluated,

Table 1
Optimal Threshold and Total (Training + Testing Sets) Error Chart for various Window Sizes.

Window Size	θ_1	θ_2	# of False Alarms	# of Mis-detections	Total % age Error
10-s	1.011	1.049	5	4	8.04%
5-s	1.010	1.051	2	4	5.36%
2-s	1.014	1.045	8	1	8.06%
1-s	1.005	1.055	5	4	8.06%
0.5-s	1.001	1.045	10	5	13.39%

where the (scalar-valued) measure ρ (see Eq. (1) in SubSection 3.2) being less than θ_1 implies pre-LBO or LBO, and being greater than θ_2 implies TAI; and stable operations otherwise. The optimal thresholds are obtained by analyzing the training data (which are 70% of the entire data) and the thresholds are tested on the remaining testing data (which are 30% of the entire data). This analysis has been over 20 trials and average values are listed in Table 1.

Since the data length needed to make these decisions is an important criterion, especially for online detection, several window lengths are considered, namely, the full data length of 10-s, as well as smaller windows of 5-s, 2-s, 1-s and 0.5-s. Table 1 lists the values of the learnt optimal thresholds, θ_1 and θ_2 . Table 1 also shows the number of total misdetected cases, (i.e., unstable signals classified as stable) and false alarms (i.e., stable cases classified as unstable) across both training and testing sets. The total percentage classification error, obtained by dividing the number of incorrectly classified cases by the total number of data time-series, is also presented in the last column of Table 1.

The results listed in Table 1 show that the proposed FFT-based algorithm works quite well in the sense that it is capable of classifying a signal into LBO, TAI or stable regimes with good accuracy (e.g., less than 10% error) for window sizes greater than 1 s long; the lowest accuracy (13.39%) is seen for the smallest window size of 0.5 s length. This is reasonable, because although the process is statistically stationary, the smallest window size might not accurately capture the system dynamics in the presence of process and measurement noise. As seen in Table 1, a 5-s data window has yielded the highest classification accuracy. The confusion matrix for the classification error in the testing set is presented in Table 2, using a window size of 5-s, where the thresholds θ_1 and θ_2 are as listed in Table 1. It is seen in Table 2 that, under this condition, there is no misclassification of the LBO and stable regime, with a low mis-detection rate (e.g., misdetecting only 2 out of 19 test cases for the TAI regime). Interestingly, the performance of 10-s window is not as good as that of the 5-s window. A possible rationale for this outcome is that the FFT is a signal averaging method, which tends to partially average the transient signals beyond the 5-s duration, consequently yielding less accurate results.

This paper has also investigated the possibility of having a common optimal threshold across a range of window lengths. This common threshold is identified by taking the mean of thresholds obtained for the five different window lengths. Thus, the global threshold is computed as $\theta_1^* = 1.010$ and $\theta_2^* = 1.049$. The generated errors and number of false alarms and mis-detected cases over both training and testing data are listed in Table 3. It is seen that, with even this common threshold over all window lengths, the maximum error is limited to 14.29% error with a maximum of 16 mis-classifications. The results are considered to be

Table 2
Confusion matrix for combustor regime detection in testing set for data-length = 5-s, $\theta_1 = 1.010$ and $\theta_2 = 1.051$.

	Classified Stable	Classified TAI	Classified LBO
Actually Stable	100%	0%	0%
Actually TAI	10.53%	89.47%	0%
Actually LBO	0%	0%	100.00%

Table 3
Error Chart (Training + Testing Sets) for various Window Sizes for Common Threshold of $\theta_1^* = 1.010$ and $\theta_2^* = 1.049$.

Window Size	# of False Alarms	# of Mis-detections	Total % age Error
10-s	4	5	8.04%
5-s	5	5	8.93%
2-s	8	6	12.50%
1-s	10	1	9.82%
0.5-s	8	8	14.29%

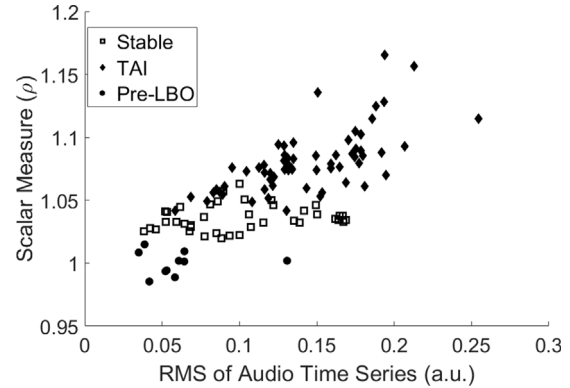


Fig. 6. Scatter plot showing the true regime as a function of the signal RMS value and the (scalar-valued) measure ρ (see Eq. (1)), where “a.u.” in the abscissa indicates arbitrary units.

reasonably accurate, given that this algorithm is of low computational complexity and uses nothing but the audio signal data obtained from a commercially available microphone. As expected, the lowest accuracy is seen for the smallest window length. Since the results in Table 3 are less accurate than those in Table 1, it is concluded that the optimal threshold for a selected fixed-window-length should be used only under severe time-constraints of real-time monitoring.

Several researchers (e.g., Santavicca et al. [31]) have used root mean square (RMS) values of the signal (typically pressure signals) as a classification criterion. Fig. 6 presents plots of the experimentally observed condition (i.e., ground truth), with the signal RMS as the abscissa and the (scalar-valued) measure ρ (see Eq. (1)) as the ordinate for 5-s data (see Table 2). It is seen that the RMS does not form a very good basis for distinguishing various operational regimes, probably due to the following fact. Under two different operating conditions, one which is TAI (e.g., having low air flow rate and low ϕ) and the other which is stable (e.g., having high air flow rate and low ϕ), computed RMS values of the acoustic signal could be indistinguishable due to measurement noise in the flow rate.

The computational complexity of the proposed FFT-based algorithm is insignificant, because it primarily computes the FFT, followed by a few algebraic operations. The FFT computation acts as the speed-determining factor in this algorithm, because the execution times to generate FFT of 10-s, 5-s, 2-s, 1-s and 0.5-s windows of data are approximately 4.8 ms, 2.3 ms, 1.2 ms, 0.8 ms and 0.6 ms, respectively, on a single processor of a DELL Precision Tower 7910 Workstation running an Intel® Xeon® E5-2670 CPU. Typically the growth of combustion instability takes place within a time interval in the order of 0.5–1 s [33,34] and the decay into LBO is a slower process. Thus, for online detection, the proposed FFT-based algorithm is sufficiently fast and much less computationally complex than many other data-driven methods.

4.4. Unsteady signal analysis

This subsection demonstrates viability of the proposed algorithm for

online classification of LBO and TAI from time series of audio signals. Transient data were collected from the experimental apparatus in Fig. 1, where the equivalence ratio (ϕ) was gradually varied over a long time by keeping the air flow rate (\dot{Q}_A) constant while varying the fuel flow rate (\dot{Q}_F) at steps of 0.1 SLPM. At each ϕ , the fuel flow rate was held constant for 10 s before changing to the next value of ϕ .

For testing the algorithm in an online setting, the time-series data are windowed at 10 Hz, i.e. 10 windows per second, while each window is of 2-s length. The reason for choosing this window length is driven by the following requirements.

1. A sufficient window length is needed for generation of an FFT that can yield a good metric with low mis-detection (see Table 1).
2. Small window lengths are preferable for prompt detection and real-time control.

The 2-s window length optimizes both of the above requirements. Furthermore, the data are sampled every 100 ms, leading to overlapping windows, which provides ample computational time for the analysis to be done. It is seen earlier that a 2-s window of data requires 1.2 ms to be analysed.

Figs. 7 and 8 show two sample cases of transience: (i) from stable operation to LBO, and (ii) from stable operation to TAI, respectively. It is seen that as the operating condition moves from stable to either TAI or LBO, the (scalar-valued) measure (ρ) increases or decreases accordingly. Using the learnt threshold values (see Table 1), online detection and classification can be performed to appropriately identify the change in regime with low numbers of misdetections and false alarms. The detected regimes, shown in the bottom plate of each of Figs. 7 and 8, are also indicated. It is clearly seen in Fig. 7 how a drop in ρ signifies approach to LBO and detects the imminent LBO long before it happens (at the end of the signal). Similarly, Fig. 8 shows that an increase in ρ indicates an approaching TAI.

It is concluded from Figs. 7 and 8 that the proposed method can detect and identify acoustic precursors in real time, which would lead to prediction of the impending onset of TAI and LBO by capturing a change in the scalar-valued metric (ρ) before the occurrence of the

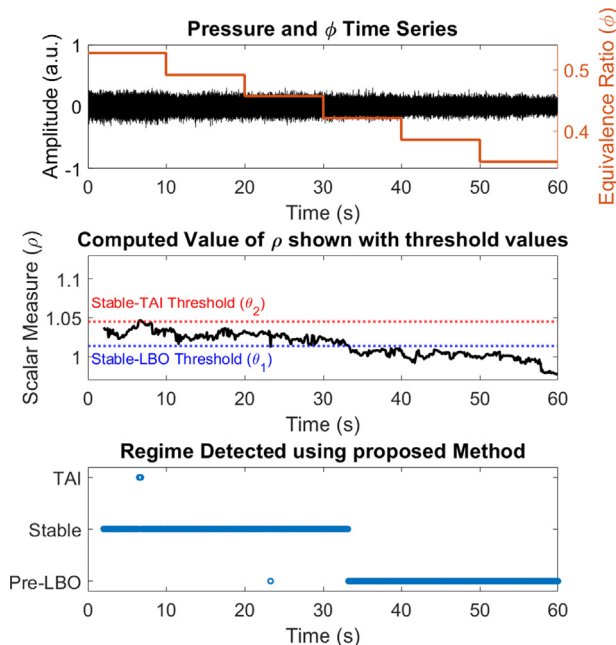


Fig. 7. (top) Pressure time series and Equivalence Ratio (ϕ) when system goes from Stable to LBO conditions, where “a.u.” in the ordinate indicates arbitrary units; (middle) Computed value of measure (ρ) shown along with the thresholds (θ_1 and θ_2); (bottom) Detected Regime using ρ and thresholds.

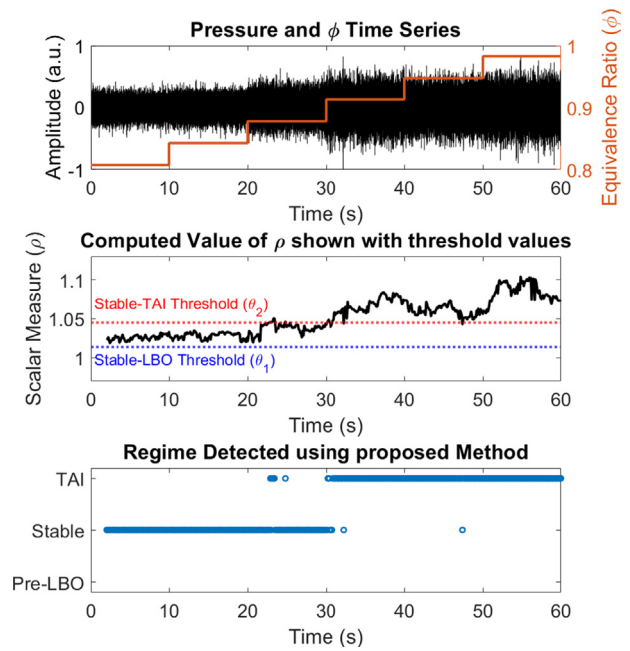


Fig. 8. (top) Pressure time series and Equivalence Ratio (ϕ) when system goes from Stable to TAI conditions, where “a.u.” in the ordinate indicates arbitrary units; (middle) Computed value of measure (ρ) shown along with the thresholds (θ_1 and θ_2); (bottom) Detected Regime using ρ and thresholds.

(LBO or TAI) event. This is seen in Fig. 7, where LBO occurs at $\phi = 0.351$ but the algorithm can predict the onset at $\phi = 0.421$. Similarly, full blown TAI is observed at $\phi = 0.912$ while the imminent change is predicted at $\phi = 0.878$ as seen in Fig. 8.

The operating principle of the proposed method relies on the following entities: (i) prior (possibly physics-based) knowledge of the dominant frequency(s) during LBO and TAI; and (ii) the scalar measure (ρ) (see Eq. (1)), which identifies the dominant frequency(s) in the LBO or TAI regime as compared to no dominant frequency in the stable regime. The transition into LBO begins at equivalence ratios higher than the LBO limit, which in turn shows up as a steady increase in the LBO peak frequency(s). The proposed scalar indicator is able to capture this event, which leads to an early assessment of a forthcoming LBO, thus ‘predicting’ its occurrence. For TAI, the problem is more difficult because the transition to TAI is less gradual; however, in conditions very near to TAI, the TAI frequency(s) begin(s) to appear with larger amplitudes. Thus, it is possible to have early detection of a forthcoming TAI by using the scalar measure ρ .

5. Summary, conclusions, and future work

This paper has developed and validated a computationally-efficient and easily-implementable FFT-based method for detection and classification of combustion regimes, namely, (1) lean blow out (LBO), (2) stable operation and (3) thermoacoustic instability (TAI). The underlying principle of the proposed method is built upon the physics of the combustion process and combustor acoustics, which is similar for nearly all combustor configurations. The following points summarize the highlights of this paper.

- The simple (yet robust) FFT-based method computes a scalar measure to determine which of the regimes of interest the combustion system is currently in and would tend to be in the near future.
- For the analysis, the algorithm requires only time series of audio signals that can be captured by a commercial-grade microphone, placed external to the apparatus, which eliminates the need for invasive and expensive sensors.

- The scalar measure (ρ) takes advantage of the prior knowledge about the dominant acoustic modes (or frequencies) seen during TAI and LBO, and uses simple scalar thresholds to discriminate the three regimes of interest with reasonably good accuracy.
- The proposed method has been tested for both steady-state and transient time series of audio signals obtained from a laboratory-scale swirl-stabilized combustor apparatus. The underlying algorithm is shown to be capable of detecting impending transitions to TAI or LBO by capturing the gradual growth in the dominant frequencies.

Although the proposed method is developed, tested and validated on a laboratory-scale swirl-stabilized combustor apparatus, it can be potentially extended to other combustion systems, where there exists prior knowledge about the dominant acoustic modes observed during LBO and TAI.

While further theoretical and experimental research is necessary before the proposed method can be actually implemented in industrial combustors, the near-term future work envisaged by the authors are:

- *Testing and experimental validation* of the proposed FFT-based algorithm for different conditions of the combustor, and also on other types of combustors.
- *Development of a rigorous experimental procedure* for the algorithm to identify the frequencies of importance in a data-driven fashion from an ensemble of classified data.
- *Investigation of the strength of the algorithm* in being able to provide a measure of the ‘degree of deviation’ from the nominal (stable) condition.
- *Exploration of other nonlinear regimes* in the audio signal to study the presence of possibly intermittent and chaotic behavior (e.g. [35]) and relevance of the dominant acoustic modes.

Declaration of Competing Interest

The authors declare that they have no known competing financial interests or personal relationships that could have appeared to influence the work reported in this paper.

Acknowledgments

The first author thanks Indo-US Science and Technology Forum (IUSSTF) for granting the Research Internship for Science and Engineering (RISE) scholarship for collaboration between Pennsylvania State University (PSU) and Jadavpur University (JU). The second, third and fourth authors acknowledge the RUSA 2.0 program of JU for financial support. All authors acknowledge SPARC, MHRD, Govt. of India for supporting collaboration between PSU and JU through its Project No. P1065. The work reported here has also been supported in part by the U.S. Air Force Office of Scientific Research (AFOSR) under Grant Nos. FA9550-15-1-0400 and FA9550-18-1-0135 in the area of dynamic data-driven application systems (DDDAS). Opinions, findings, conclusions or recommendations expressed in this publication are those of the authors and do not necessarily reflect the views of the sponsoring agencies.

References

- [1] M.H. Baumgärtner, T. Sattelmayer, Improvement of the turn-down ratio of gas turbines by autothermal on board syngas generation, *J. Global Power Propul. Soc.* 1 (2017) 55–70.
- [2] L. Rayleigh, *The Theory of Sound*, Dover Publications, 1945.
- [3] S. Candel, Combustion dynamics and control: Progress and challenges, *Proc. Combust. Inst.* 29 (2002) 1–28.
- [4] K.R. McManus, T. Poinot, S.M. Candel, A review of active control of combustion instabilities, *Prog. Energy Combust. Sci.* 19 (1993) 1–29.
- [5] F.E.C. Culick, *Combustion Instabilities in Propulsion Systems*, Springer, Netherlands, Dordrecht, 1996, pp. 173–241.
- [6] A.H. Lefebvre, *Gas Turbine Combustion*, second ed., CRC Press Taylor & Francis Group, Boca Raton, FL, 1998.
- [7] T.M. Muruganandam, S. Nair, D. Scarborough, Y. Neumeier, J. Jagoda, T. Lieuwen, J. Seitzman, B. Zinn, Active control of lean blowout for turbine engine combustors, *J. Propul. Power* 21 (5) (2005) 807–814.
- [8] P. Allison, K. Frederickson, J.W. Kirik, R.D. Rockwell, W.R. Lempert, J.A. Sutton, Investigation of flame structure and combustion dynamics using CH_2O plif and high-speed chemiluminescence in a premixed dual-mode scramjet combustor, in: 54th AIAA Aerospace Sciences Meeting, 2016, p. 0441.
- [9] T. Yi, E.J. Gutmark, Real-time prediction of incipient lean blowout in gas turbine combustors, *AIAA J.* 45 (7) (2007) 1734–1739.
- [10] F. Li, L. Xu, M. Du, L. Yang, Z. Cao, Ion current sensing-based lean blowout detection for a pulse combustor, *Combust. Flame* 176 (2017) 263–271.
- [11] L. Chang, Z. Cao, B. Fu, Y. Lin, L. Xu, Lean blowout detection for bluff-body stabilized flame, *Fuel* 266 (2020) 117008.
- [12] S. De, A. Biswas, A. Bhattacharya, A. Mukhopadhyay, S. Sen, Use of flame color and chemiluminescence for early detection of lean blowout in gas turbine combustors at different levels of fuel-air premixing, *Combust. Sci. Technol.* (2019) 1–25, <https://doi.org/10.1080/00102202.2019.1604514>.
- [13] S. De, A. Bhattacharya, S. Mondal, A. Mukhopadhyay, S. Sen, Application of recurrence quantification analysis for early detection of lean blowout in a swirl-stabilized dump combustor, *Chaos: Interdiscipl. J. Nonlinear Sci.* 30 (4) (2020) 043115.
- [14] V. Nair, G. Thampi, S. Karuppusamy, S. Gopalan, R.I. Sujith, Loss of chaos in combustion noise as a precursor of impending combustion instability, *Int. J. Spray Combust. Dyn.* 5 (4) (2013) 273–290.
- [15] M. Murugesan, R.I. Sujith, Combustion noise is scale-free: transition from scale-free to order at the onset of thermoacoustic instability, *J. Fluid Mech.* 772 (2015) 225–245.
- [16] L. Lacasa, B. Luque, F. Ballesteros, J. Luque, J.C. Nuño, From time series to complex networks: the visibility graph, *Proc. Nat. Acad. Sci.* 105 (13) (2008) 4972–4975.
- [17] T. Kobayashi, S. Murayama, T. Hachijo, H. Gotoda, Early detection of thermoacoustic combustion instability using a methodology combining complex networks and machine learning, *Phys. Rev. Appl.* 11 (6) (2019) 064034.
- [18] U. Sen, T. Gangopadhyay, C. Bhattacharya, A. Mukhopadhyay, S. Sen, Dynamic characterization of a ducted inverse diffusion flame using recurrence analysis, *Combust. Sci. Technol.* 190 (1) (2018) 32–56.
- [19] S. Mondal, C. Bhattacharya, P. Chattopadhyay, A. Mukhopadhyay, A. Ray, Prediction of thermoacoustic instabilities in a premixed combustor based on fft-based dynamic characterization, in: 53rd AIAA/SAE/ASEE Joint Propulsion Conference, 2017.
- [20] K. Murphy, *Machine Learning: A Probabilistic Perspective*, MIT Press, Cambridge, MA, USA, 2012.
- [21] S. Sarkar, S.R. Chakravarthy, V. Ramanan, A. Ray, Dynamic data-driven prediction of instability in a swirl-stabilized combustor, *Int. J. Spray Combust. Dyn.* 8 (4) (2016) 235–253.
- [22] S. Sarkar, K.G. Lore, S. Sarkar, V. Ramanan, S.R. Chakravarthy, S. Phoha, Early detection of combustion instability from hi-speed flame images via deep learning and symbolic time series analysis, in: Annual Conference of the Prognostics and Health Management Society, 2015.
- [23] L.R. Rabiner, A tutorial on hidden Markov models and selected applications in speech recognition, *Proc. IEEE* 77 (2) (1989) 257–286.
- [24] S. Mondal, N. Ghalyan, A. Ray, A. Mukhopadhyay, Early detection of thermoacoustic instabilities using hidden Markov models, *Combust. Sci. Technol.* (2018) 1–28.
- [25] N. Hosseini, V. Kornilov, I. Lopez Arteaga, W. Polifke, O. Teerling, L. de Goeij, Intrinsic thermoacoustic modes and their interplay with acoustic modes in a rijke burner, *Int. J. Spray Combust. Dyn.* 10 (4) (2018) 315–325.
- [26] T. Emmert, S. Bomberg, S. Jaensch, W. Polifke, Acoustic and intrinsic thermoacoustic modes of a premixed combustor, *Proc. Combust. Inst.* 36 (3) (2017) 3835–3842.
- [27] S. Candel, D. Durox, T. Schuller, J.-F. Bourgoignie, J.P. Moeck, Dynamics of swirling flames, *Ann. Rev. Fluid Mech.* 46 (2014) 147–173.
- [28] M. Bauerheim, M. Cazalens, T. Poinot, A theoretical study of mean azimuthal flow and asymmetry effects on thermoacoustic modes in annular combustors, *Proc. Combust. Inst.* 35 (3) (2015) 3219–3227.
- [29] Gas India Ltd., Technical specifications: Properties of propane, butane and LPG. URL www.gasindia.in/technical-specification.html.
- [30] T.C. Lieuwen, Statistical characteristics of pressure oscillations in a premixed combustor, *J. Sound Vib.* 260 (1) (2003) 3–17.
- [31] J.G. Lee, D.A. Santavicca, Experimental diagnostics for the study of combustion instabilities in lean premixed combustors, *J. Propul. Power* 19 (2003) 735–750.
- [32] A.D. Whalen, Hypothesis testing, in: *Detection of Signals in Noise*, Academic Press, 1971, pp. 125–154 (Chapter 5).
- [33] W. Culler, X. Chen, J. Samarasinghe, S. Peluso, D. Santavicca, J. O’Connor, The effect of variable fuel staging transients on self-excited instabilities in a multiple-nozzle combustor, *Combust. Flame* 194 (2018) 472–484.
- [34] C. Bhattacharya, S. Mondal, A. Ray, A. Mukhopadhyay, Reduced-order modeling of thermoacoustic instabilities in a two-heater Rijke tube, *Combust. Theory Model.* (2020), <https://doi.org/10.1080/13647830.2020.1714080>.
- [35] Y. Sun, Z. Rao, D. Zhao, B. Wang, D. Sun, X. Sun, Characterizing nonlinear dynamic features of self-sustained thermoacoustic oscillations in a premixed swirling combustor, *Appl. Energy* 264 (2020) 114698.